

# Electrocatalytic Currents from Single Enzyme Molecules

Alina N. Sekretaryova,<sup>\*,†</sup> Mikhail Yu. Vagin,<sup>†,‡</sup> Anthony P. F. Turner,<sup>†</sup> and Mats Eriksson<sup>†</sup>

<sup>†</sup>Department of Physics, Chemistry and Biology, Linköping University, SE-581 83, Linköping, Sweden

<sup>‡</sup>Department of Science and Technology, Linköping University, SE-601 74, Norrköping, Sweden

**S** Supporting Information

**ABSTRACT:** Single molecule enzymology provides an opportunity to examine details of enzyme mechanisms that are not distinguishable in biomolecule ensemble studies. Here we report, for the first time, detection of the current produced in an electrocatalytic reaction by a single redox enzyme molecule when it collides with an ultramicroelectrode. The catalytic process provides amplification of the current from electron-transfer events at the catalyst leading to a measurable current. This new methodology monitors turnover of a single enzyme molecule. The methodology might complement existing single molecule techniques, giving further insights into enzymatic mechanisms and filling the gap between fundamental understanding of biocatalytic processes and their potential for bioenergy production.

The “single-molecule toolkit” for enzyme investigation has so far involved techniques based on mechanical or fluorescence transduction mechanisms.<sup>1–4</sup> Electrochemical transduction to monitor the electrocatalytic current from a single enzyme molecule has, however, not previously been demonstrated.<sup>5</sup> Redox enzymes are key in a number of essential biological processes such as bioenergetics, elemental cycles, and metabolic processes. Laccase was used as a model enzyme in our studies. It is one of the earliest described redox enzymes and has been structurally well characterized.<sup>6</sup> The enzyme catalyzes the oxidation of a wide range of organic substrates concomitant with the four-electron oxygen reduction reaction (ORR),<sup>7</sup> considered to be a limiting element in oxygen-associated energy conversion.<sup>8</sup> The active site of the enzyme has four copper atoms: a type 1 (T1) Cu site and a trinuclear Cu site (TNC), which consists of a mononuclear type 2 (T2) and an antiferromagnetically coupled binuclear type 3 (T3) site. Oxidation of organic substrates occurs via a so-called ‘ping-pong’ mechanism. Substrates are oxidized near the solvent accessible T1 site, and then electrons are transferred through the protein, via a Cys-His pathway, over a distance of ~12 Å to the TNC site where the ORR occurs.<sup>9,10</sup> One of the key characteristics of laccases from different sources is the standard redox potential of their redox centers, which determines their catalytic efficiency toward reducing substrates. The redox potential of the T1 center for the *Trametes versicolor* laccase, used in this study, has been reported to be about 780 mV vs the normal hydrogen electrode (NHE), and the redox potential of the T2 site is about 400 mV vs NHE.<sup>11</sup> Laccase offers the possibility of direct electron transfer (DET) between its active

site and an electrode.<sup>10</sup> In this case, the electrode replaces the substrate oxidized by laccase.

Attempts to detect the catalytic current from a single redox enzyme molecule have been made by downscaling protein-film voltammetry (PFV)<sup>12,13</sup> to enzyme measurements on nano-electrodes. This approach, however, currently only allows a resolution of 8–46 biomolecules.<sup>14</sup> In our study, we used a novel approach of collision-based bioelectrocatalysis (Figure 1)

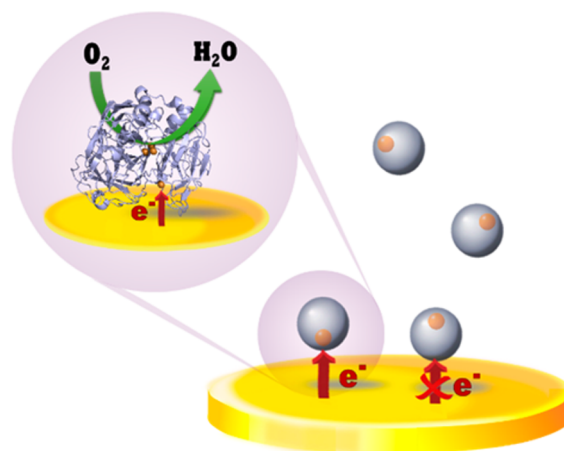


**Figure 1.** Scheme showing the principle of detection of the catalytic current from a single enzyme molecule. When the enzyme molecule (shown as a gray ball) collides with the AuUME in such a geometry that its active center (shown as an orange ball inside the molecule) is close to the electrode surface, direct electron transfer from the electrode to the enzyme occurs, followed by reduction of molecular oxygen to water. The process is detected as a reduction current. In the case where the geometry of the active center of the enzyme molecule is less favorable, no current signal is observed.

to monitor the electrocatalytic current from single redox enzyme molecules in solution. The catalytic process provides amplification of the current from electron-transfer events at the catalyst leading to a measurable current.<sup>15</sup> Collision-based electrochemistry has recently been extensively used for characterization of single catalytic nanoparticles,<sup>16</sup> for studying adsorption of proteins and DNA strands,<sup>17</sup> and for detection of redox protein molecules assembled on the surface of graphene oxide flakes,<sup>18</sup> but not for monitoring catalytic currents produced by individual molecules.

Received: December 16, 2015

Published: February 12, 2016

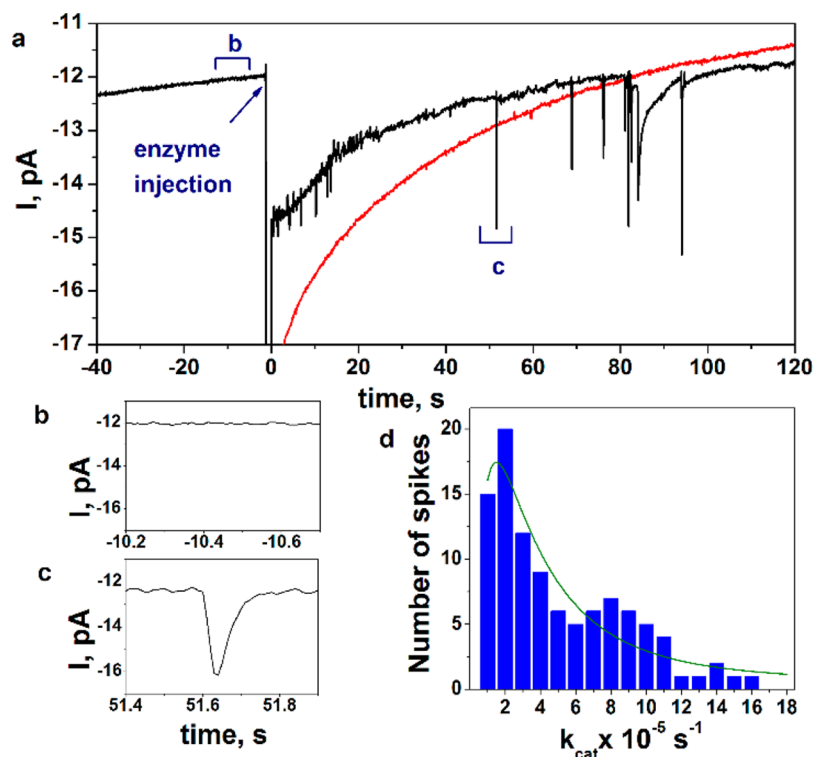


**Figure 2. Monitoring the electrocatalytic current from individual enzyme molecules.** (a). Amperometric  $i-t$  curves in the presence of  $0.1 \text{ U mL}^{-1}$  enzyme solution in a deoxygenated solution (red) and in an oxygen containing solution (black). The AuUME was biased at  $+0.210 \text{ V}$  vs NHE over the entire experimental time. (b and c) Magnified  $i-t$  curves, of the parts indicated in a, showing the background and a clear spike-shaped response, respectively. (d) Distribution of turnover rates of the enzyme molecules, calculated from the collision experiment using the peak height value, fitted by log-normal statistics. The mean value is  $(3.8 \pm 1.1) \times 10^5 \text{ s}^{-1}$ . Experimental conditions were: pH 5.0 (0.1 M acetate buffer),  $T = 20 \text{ }^\circ\text{C}$ .

Chronoamperometry was used to observe DET between a single enzyme globule and a gold ultramicroelectrode (AuUME) at  $+0.210 \text{ V}$  vs NHE (Figure 2a, Figure S1). Before addition of the enzyme solution to the cell, we observed a current noise in 0.1 M acetate buffer (pH 5.0) of  $\pm 0.1 \text{ pA}$  (Figure 2b). After addition of the enzyme solution to a final concentration of  $0.1 \text{ U mL}^{-1}$  current spikes of several pA were observed, which is close to the value predicted by the mass-transfer limiting current generated at individual nanoparticles (Supporting Note 1). When an enzyme molecule collides with the electrode, it randomly adsorbs onto the electrode surface.<sup>17</sup> In the case where the adsorption geometry is suitable for electrode transfer between the enzyme and the electrode (Figure 1), an electrocatalytic ORR occurs and produces a current due to the enzyme turning over. The signals observed were in the form of spikes rather than steady-state current steps, probably due to partial denaturation or structural changes of the enzyme molecule as a result of the adsorption process.<sup>19</sup> To confirm that these spikes are due to DET between an enzyme molecule and the electrode, a control experiment was performed under identical experimental conditions, but without oxygen (red curve, Figure 2a). No spikes were observed in the control experiment. Addition of an enzyme inhibitor, NaF solution,<sup>10</sup> to the enzyme solution also led to disappearance of the current spikes after approximately 30 s of inhibition, confirming that the observed response is the result of enzyme catalytic activity (Figure S2). To demonstrate that there is no aggregation of enzyme molecules in the solution and that the observed current spikes are mainly due to single molecule collisions, dynamic light scattering (DLS) measurements of the particle size in acetate buffer were performed (Figure S3).

Although the enzyme concentration was 10–100 hundred times higher in the DLS measurements than in the electrochemical experiment, no significant aggregation was observed. We observed a narrow particle size distribution with a mean value of  $\sim 6 \text{ nm}$ , which is in agreement with the reported size of the *Trametes versicolor* laccase molecule.<sup>6</sup> Moreover, the zeta potential of the enzyme globule in the buffer solution was measured and shown to have a slightly negative value,  $-11 \pm 3 \text{ mV}$ , thus discouraging aggregation of the enzyme globules.

The spike frequency in the chronoamperometry experiments is related to diffusion of enzyme molecules to the electrode.<sup>20</sup> The diffusion coefficient of enzyme molecules can be calculated using the generalized Stokes–Einstein equation. However, in diluted enzymatic solutions without molecule aggregation, the interaction between the particles can be neglected and the diffusion coefficient,  $D_E$ , can be estimated using:<sup>21</sup>

$$D_E = \frac{k_B T}{6\pi\eta r_E} \quad (1)$$

where  $k_B$  is the Boltzmann constant,  $T$  is the absolute temperature,  $\eta$  is the viscosity of water ( $8.94 \times 10^{-4} \text{ Pa}\cdot\text{s}$  at  $25 \text{ }^\circ\text{C}$ ),<sup>20</sup> and  $r_E$  is the radius of the enzyme molecule. The diffusion coefficient of the enzyme molecule according to eq 1 is  $8.14 \times 10^{-7} \text{ cm}^2 \text{ s}^{-1}$ . The collision frequency due to diffusion can be calculated by:<sup>20</sup>

$$f = 4D_E C_E r_{\text{elec}} N_A \quad (2)$$

where  $C_E$  is the enzyme concentration,  $r_{\text{elec}}$  is the radius of the AuUME, and  $N_A$  is Avogadro's number. The predicted collision frequency is 0.17 MHz. Assuming that all enzymes stick to the electrode surface with a sticking coefficient of 1,<sup>17</sup> independent

of the enzyme coverage and the presence of other adsorbates, it would take about 25 s to cover the electrode surface at this collision frequency. In our experiments, we observed that the peaks disappeared approximately 100–150 s after the addition of the enzyme solution. Assuming that this indicates the formation of a full monolayer, the results indicate a somewhat lower sticking probability than one, on average. By adding results from more than 20 measurements, a decrease of the spike frequency with time can be discerned, indicating that the enzyme sticking probability decreases with increasing enzyme coverage. The data obtained may be influenced by the presence of impurities in the enzyme preparation, and hence we did not attempt to accurately model the process of enzyme adsorption using this information. The experimentally observed spike frequency in acetate buffer was 0.18 Hz, suggesting that very few of the enzyme molecules are in conformations suited for DET, that only a small part of the enzyme molecule surface area is available for the electron coupling with the electrode or that impurities influence the adsorption. The collision frequency measured in 0.01 M phosphate buffer (pH 7.4) was much lower, 0.03 Hz, which reflects a turnover rate decrease. This was probably due to the low stability of laccase at neutral pH, which is related to interactions between hydroxyl ions and the TNC leading to enzyme deactivation (Figure S4).

By measuring the height of the catalytic current spikes (Figure 2c) and assuming that four electrons are needed for reduction of one oxygen molecule, we were able to calculate the maximum turnover numbers ( $k_{\text{cat}}$ ) of the individual enzyme molecules when they interact with the electrode (Supporting Note 2). Figure S4 shows the dependence of the current spikes (size and frequency) on pH. The observed spikes, and therefore the turnover rates, are largest at pH 4.0–5.0 and decrease with increasing pH of the buffer solution. Figure 2d shows the turnover number distribution for a large number of molecule–electrode interactions at pH 5.0. The experimental data can be fitted by a log-normal distribution with an arithmetic mean of  $3.8 \times 10^5 \text{ s}^{-1}$  and has a broad range of turnover rate fluctuations. Adsorption of the enzyme molecules on the electrode surface during the collisions led to partial denaturation of the enzyme in the process of turnover. The number of turnovers per enzyme molecule can be estimated using the mean value of  $k_{\text{cat}}$  multiplied by the typical duration of the spike, which is  $\sim 0.05 \text{ s}$ . This estimation gives a total number of turnovers of  $2 \times 10^4$  for a typical collision.

The observed large variation of the turnover number supports previously obtained results based on fluorescence measurements.<sup>23,24</sup> The distribution may be caused by intrinsic and extrinsic factors.<sup>25</sup> First, the adsorption geometry might influence the observed turnover number in the case where electron transfer from the electrode to the enzyme molecule is the rate-determining step. Second, DET between an AuUME and an enzyme molecule is strongly dependent on the surface state of the electrode.<sup>10</sup>

It has been suggested<sup>10</sup> that the intermolecular electron transfer from the electrode to the T1 redox center of the enzyme in its native condition is the rate-determining step in the overall catalytic process, involving subsequent intramolecular electron transfer (IET) between the T1 and the T2/T3 redox centers<sup>9,26</sup> and finally ORR at the T2/T3 center<sup>6</sup> (Figure 3a). Hence, the application of an overpotential to the electrode can change the rate-determining step from intermolecular electron transfer to IET (Supporting Note 3). Figure 3b shows the dependence of the observed catalytic currents

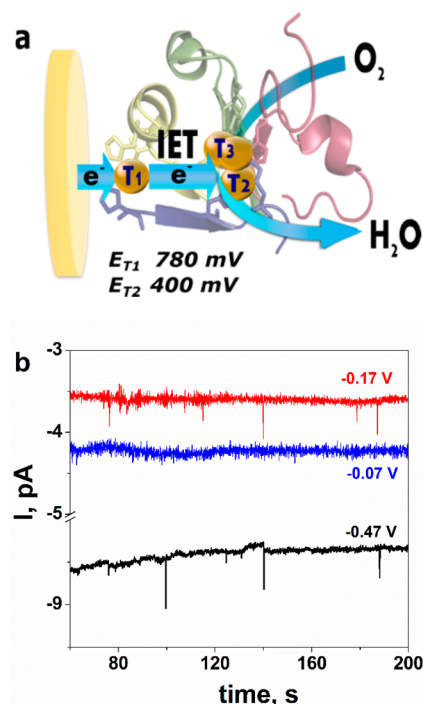


**Figure 3.** Influence of the potential on the observed electron transfer rate. (a) Scheme showing the electron transfer pathway from the electrode to molecular oxygen in the solution. The values refer to the redox potentials of the T1 ( $E_{T1}$ ) and T2 ( $E_{T2}$ ) centers for the *Trametes versicolor* laccase vs NHE. (b) Amperometric  $i-t$  curves in the presence of  $0.1 \text{ U mL}^{-1}$  enzyme solution in an oxygen containing solution. The AuUME was biased at different overpotentials (applied potential minus T1 redox potential) of  $-0.07 \text{ V}$  (blue curve),  $-0.17 \text{ V}$  (red curve), and  $-0.47 \text{ V}$  (black curve) vs NHE. Experimental conditions: pH 5.0 (0.1 M acetate buffer),  $T = 20 \text{ }^\circ\text{C}$ .

from single enzyme molecules on the applied potential. The size of the observed spikes revealed an independence of the potential at high cathodic overpotentials indicating IET current limitation. No spikes were detected at small overpotentials (due to the insensitivity of amperometry to the small catalytic currents at the close-to-equilibrium conditions in this experimental setup). Thus, the method can be used to estimate the redox potential of the primary electron acceptor site communicating directly with the electrode, assuming that the potential of the T1 site correlates with the catalytic potential.<sup>27</sup>

While the mechanism of oxygen reduction in laccases is known, the detailed process of IET has remained unclear,<sup>9</sup> since attempts to measure the IET transfer rate from T1 to TNC have resulted in low and noncatalytically relevant values, maybe due to the experimental conditions of those experiments.<sup>7</sup> It has, however, been proposed that IET could be fast.<sup>9,22</sup> Recent microsecond freeze-hyper quench studies showed experimental IET rates in laccases of  $>2.5 \times 10^4 \text{ s}^{-1}$ .<sup>28</sup> Our studies at high overpotential, when IET is the limiting process, also revealed even higher rates (Figure 2d).

The measurements of Figure 2 were performed at an overpotential of  $-0.57 \text{ V}$ , and we therefore assume that the observed  $k_{\text{cat}}$  fluctuations are related mainly to the fluctuations in enzyme conformations<sup>23</sup> and thermodynamics of the intramolecular electron transfer.<sup>25</sup> Using the semiclassical Marcus theory and the obtained mean value of  $k_{\text{cat}}$ , an estimated value of 0.20 eV for the activation energy was calculated. The reorganization energy for intramolecular

electron transfer was calculated to be 0.72 eV, which is within the range calculated theoretically<sup>26</sup> (Supporting Note 4).

In summary, we have demonstrated the possibility to monitor electrocatalytic events from single laccase molecules. This methodology allows single enzyme molecules to be studied electrochemically and may be applicable to other redox enzymes with high catalytic activity and could thus complement the “single molecule toolkit”. We believe that this methodology, when applied to various more purified enzymes, will lead to new important insights into enzymatic mechanisms and fill the gap between fundamental understanding of biocatalytic processes and their potential for bioenergy production.

## ■ ASSOCIATED CONTENT

### 📄 Supporting Information

The Supporting Information is available free of charge on the ACS Publications website at DOI: [10.1021/jacs.5b13149](https://doi.org/10.1021/jacs.5b13149).

Experimental details, including data analysis, and all calculations (PDF)

## ■ AUTHOR INFORMATION

### Corresponding Author

\*[alina.sekretareva@liu.se](mailto:alina.sekretareva@liu.se)

### Notes

The authors declare no competing financial interest.

## ■ ACKNOWLEDGMENTS

The authors would like to thank The Swedish research council Formas (245-2010-1062), the research center Security Link (VINNOVA 2009-00966), and the Centre in Nano Science and Technology (CeNano, Linköping University) for financial support.

## ■ REFERENCES

- (1) Walter, N. G.; Huang, C. Y.; Manzo, A. J.; Sobhy, M. A. *Nat. Methods* **2008**, *5*, 475–489.
- (2) Chen, Q.; Groote, R.; Schonherr, H.; Vancso, G. J. *Chem. Soc. Rev.* **2009**, *38*, 2671–2683.
- (3) Smiley, R. D.; Hammes, G. G. *Chem. Rev.* **2006**, *106*, 3080–3094.
- (4) Lu, H. P. *Chem. Soc. Rev.* **2014**, *43*, 1118–1143.
- (5) Mathwig, K.; Aartsma, T. J.; Canters, G. W.; Lemay, S. G. *Annu. Rev. Anal. Chem.* **2014**, *7* (7), 383–404.
- (6) Piontek, K.; Antorini, M.; Choinowski, T. J. *Biol. Chem.* **2002**, *277*, 37663–37669.
- (7) Farver, O.; Wherland, S.; Koroleva, O.; Loginov, D. S.; Pecht, I. *FEBS J.* **2011**, *278*, 3463–3471.
- (8) Whittingham, M. S. *Chem. Rev.* **2004**, *104*, 4271–4301.
- (9) Heppner, D. E.; Kjaergaard, C. H.; Solomon, E. I. *J. Am. Chem. Soc.* **2014**, *136*, 17788–17801.
- (10) Shleev, S.; Tkac, J.; Christenson, A.; Ruzgas, T.; Yaropolov, A. I.; Whittaker, J. W.; Gorton, L. *Biosens. Bioelectron.* **2005**, *20*, 2517–2554.
- (11) Ivnitski, D.; Atanassov, P. *Electroanalysis* **2007**, *19*, 2307–2313.
- (12) Armstrong, F. A.; Heering, H. A.; Hirst, J. *Chem. Soc. Rev.* **1997**, *26*, 169–179.
- (13) Armstrong, F. A. *J. Chem. Soc., Dalton Trans.* **2002**, 661–671.
- (14) Hoeben, F. J. M.; Meijer, F. S.; Dekker, C.; Albracht, S. P. J.; Heering, H. A.; Lemay, S. G. *ACS Nano* **2008**, *2*, 2497–2504.
- (15) Xiao, X. Y.; Bard, A. J. *J. Am. Chem. Soc.* **2007**, *129*, 9610–9612.
- (16) Cheng, W.; Compton, R. G. *TrAC, Trends Anal. Chem.* **2014**, *58*, 79–89.
- (17) Dick, J. E.; Renault, C.; Bard, A. J. *J. Am. Chem. Soc.* **2015**, *137*, 8376–8379.
- (18) Li, D.; Liu, J.; Barrow, C. J.; Yang, W. *Chem. Commun.* **2014**, *50*, 8197–8200.

(19) Murgida, D. H.; Hildebrandt, P. *Phys. Chem. Chem. Phys.* **2005**, *7*, 3773–3784.

(20) Kim, B.-K.; Kim, J.; Bard, A. J. *J. Am. Chem. Soc.* **2015**, *137*, 2343–2349.

(21) Bowen, W. R.; Mongruel, A. *Colloids Surf, A* **1998**, *138*, 161–172.

(22) Solomon, E. I.; Sundaram, U. M.; Machonkin, T. E. *Chem. Rev.* **1996**, *96*, 2563–2605.

(23) English, B. P.; Min, W.; van Oijen, A. M.; Lee, K. T.; Luo, G. B.; Sun, H. Y.; Cherayil, B. J.; Kou, S. C.; Xie, X. S. *Nat. Chem. Biol.* **2006**, *2*, 87–94.

(24) Min, W.; English, B. P.; Luo, G. B.; Cherayil, B. J.; Kou, S. C.; Xie, X. S. *Acc. Chem. Res.* **2005**, *38*, 923–931.

(25) Gupta, A.; Aartsma, T. J.; Canters, G. W. *J. Am. Chem. Soc.* **2014**, *136*, 2707–2710.

(26) Winkler, J. R.; Gray, H. B. *Chem. Rev.* **2014**, *114*, 3369–3380.

(27) Rodgers, C. J.; Blanford, C. F.; Giddens, S. R.; Skamnioti, P.; Armstrong, F. A.; Gurr, S. J. *Trends Biotechnol.* **2010**, *28*, 63–72.

(28) Matijošytė, I.; Arends, I. W. C. E.; Sheldon, R. A.; de Vries, S. *Inorg. Chim. Acta* **2008**, *361*, 1202–1206.